Mycobacterium tuberculosis Alters the Metalloprotease Activity of the COP9 Signalosome

Lia Danelishvili,[a] Lmar Babrak,[a,b] Sasha J. Rose,[a,b] Jamie Everman,[a,b] Luiz E. Bermudez[a,b]

Department of Biomedical Sciences, College of Veterinary Medicine,[a] and Department of Microbiology, College of Science,[b] Oregon State University, Corvallis, Oregon, USA

L.B. and S.J.R. contributed equally to this work.

ABSTRACT **Inhibition of apoptotic death of macrophages by *Mycobacterium tuberculosis* represents an important mechanism of virulence that results in pathogen survival both *in vitro* and *in vivo*. To identify *M. tuberculosis* virulence determinants involved in the modulation of apoptosis, we previously screened a transposon bank of mutants in human macrophages, and an *M. tuberculosis* clone with a nonfunctional Rv3354 gene was identified as incompetent to suppress apoptosis. Here, we show that the Rv3354 gene encodes a protein kinase that is secreted within mononuclear phagocytic cells and is required for *M. tuberculosis* virulence. The Rv3354 effector targets the metalloprotease (JAMM) domain within subunit 5 of the COP9 signalosome (CSN5), resulting in suppression of apoptosis and in the destabilization of CSN function and regulatory cullin-RING ubiquitin E3 enzymatic activity. Our observation suggests that alteration of the metalloprotease activity of CSN by Rv3354 possibly prevents the ubiquitin-dependent proteolysis of *M. tuberculosis*-secreted proteins.**

IMPORTANCE **Macrophage protein degradation is regulated by a protein complex called a signalosome. One of the signalosomes associated with activation of ubiquitin and protein labeling for degradation was found to interact with a secreted protein from *M. tuberculosis*, which binds to the complex and inactivates it. The interference with the ability to inactivate bacterial proteins secreted in the phagocyte cytosol may have crucial importance for bacterial survival within the phagocyte.**

Received 1 May 2014 **Accepted** 14 July 2014 **Published** 19 August 2014

Citation Danelishvili L, Babrak L, Rose SJ, Everman J, Bermudez LE. 2014. *Mycobacterium tuberculosis* alters the metalloprotease activity of the COP9 signalosome. mBio 5(4): e01278-14. doi:10.1128/mBio.01278-14.

Editor Stefan Kaufmann, Max Planck Institute for Infection Biology

Copyright © 2014 Danelishvili et al. This is an open-access article distributed under the terms of the Creative Commons Attribution-Noncommercial-ShareAlike 3.0 Unported license, which permits unrestricted noncommercial use, distribution, and reproduction in any medium, provided the original author and source are credited.

Address correspondence to Luiz E. Bermudez, Luiz.Bermudez@oregonstate.edu, or Lia Danelishvili, Lia.Danelishvili@oregonstate.edu.

Tuberculosis (TB), an ancient bacterial disease, is still one of the common infectious causes of death worldwide. *Mycobacterium tuberculosis*, the etiological agent of TB, is an intracellular organism capable of survival and replication in human macrophages. These phagocytic cells are considered the first line of immune defense responsible for the killing of many bacterial pathogens. However, *M. tuberculosis* has as its primary habitat macrophages. Studies on the interaction between *M. tuberculosis* and host cells over the last decade have revealed a limited number of pathogen-derived effector molecules that directly modulate diverse macrophage killing processes. Following phagocytosis by macrophages, *M. tuberculosis* actively subverts phagolysosome biogenesis by secreting the effectors ESAT-6/CFP10 and Sec A1/2, which block phagolysosome fusion and ATP hydrolysis, respectively (1, 2). *M. tuberculosis* also secretes the lipid phosphatase SapM, serine/threonine kinase PknG, and tyrosine phosphatase PtpA proteins, which contribute to the inhibition of the normal phagosome maturation process by altering the host signaling pathways (3–5). Study of trehalose dimycolate of *M. tuberculosis* strongly indicates that this glycolipid is involved in the impairment of phagosome trafficking at an early endosomal stage (5). Furthermore, *M. tuberculosis* is able to survive in phagocytic cells by avoiding proteolytic degradation by the autophagic pathway (6). Conversely, when autophagy is stimulated by starvation, sirolimus, or gamma interferon, *M. tuberculosis* phagosomes are acidified and delivered to lysosomes, resulting in significant reduction of viable bacteria (7). Many *M. tuberculosis* effectors involved in the autophagy process are yet to be elucidated; however, some bacterial virulence effectors, such as ESAT-6/CFP-10, have been implicated in controlling autophagy (8). The secreted enhanced intracellular survival (Eis) protein has also been suggested to play an essential role in modulating host innate responses and autophagy-mediated cell death via a reactive oxygen species-dependent pathway (9).

If macrophages fail to eradicate the intracellular pathogen via autophagy or other mechanisms, host cells will undergo apoptosis as another strategy to contain the infection. However, substantial work *in vitro* and *in vivo* has revealed that macrophages infected with virulent strains of *M. tuberculosis*, in contrast to macrophages infected with an attenuated strain, exhibit less apoptosis (10, 11). The *nuoG* gene has been implicated in the suppression of host cell apoptosis (12). Infection with *pknE* or *secA2* deletion mutants of *M. tuberculosis* induces greater apoptosis upon macrophage infection than wild-type *M. tuberculosis* (13, 14). When the *secA2*-deficient clone is complemented with secreted superoxide dismutase A (*sodA*), the antiapoptotic phenotype is restored, implicating SodA in the inhibition of apoptosis.

We previously identified several genes associated with the an-

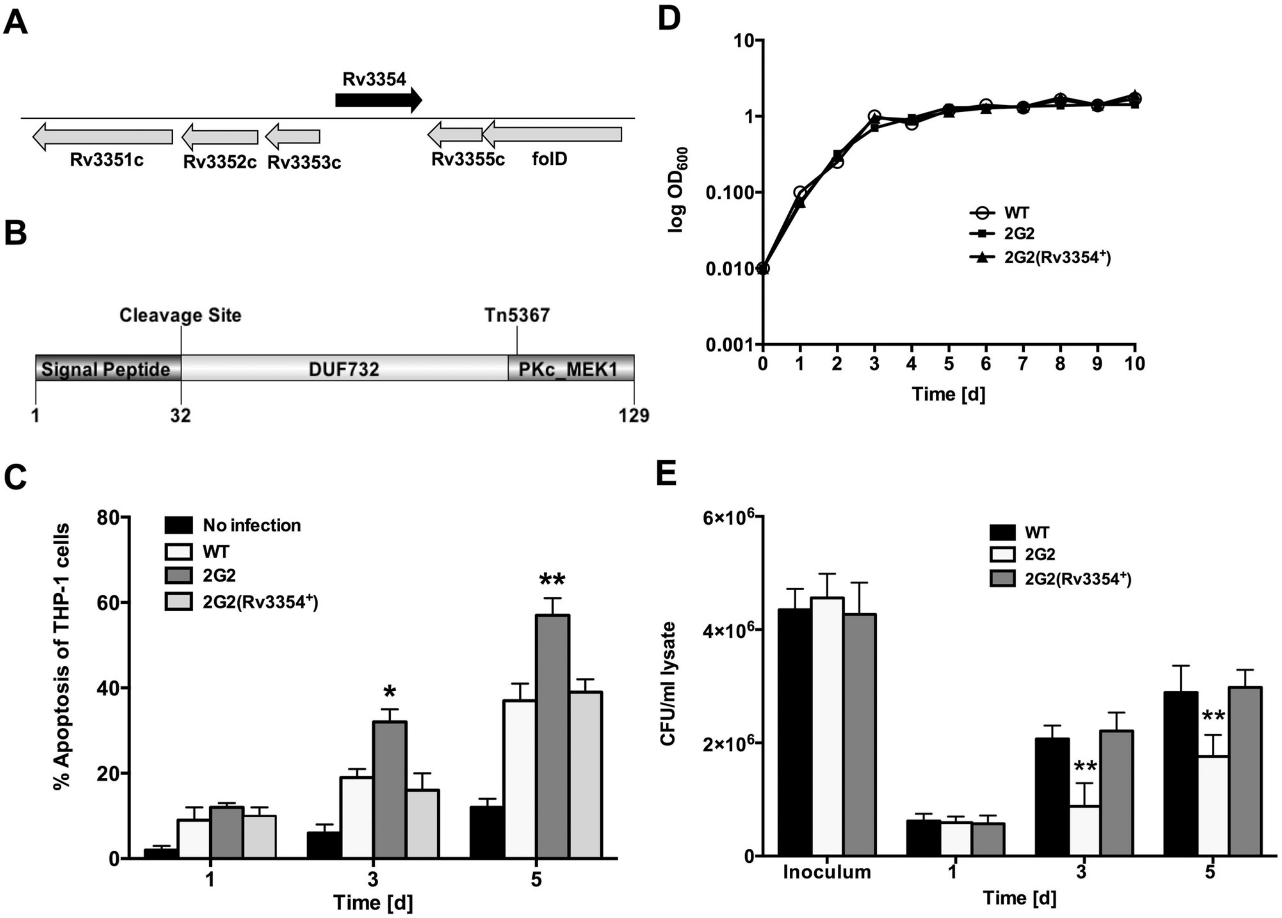

FIG 1 Inactivation of the *M. tuberculosis* Rv3354 gene. (A) Genetic organization of the Rv3354 gene in *M. tuberculosis* strain H37Rv. (B) The signal peptide, predicted domains, and Tn*5367* insertion site in the Rv3354 protein. (C) Apoptosis was analyzed in THP-1 cells infected with WT, 2G2, and 2G2 (Rv3354$^+$) in a cell death detection ELISA^{PLUS} assay (Roche). Results represent means ± standard errors of the means of three independent experiments. **, $P < 0.01$; *, $P < 0.05$, for the significance of differences between 2G2 and WT. (D) *In vitro* growth of WT, 2G2, and 2G2 (Rv3354$^+$) in aerated 7H9 medium. (E) Infection and impaired growth of 2G2 in THP-1 cells. WT, 2G2 and 2G2 (Rv3354$^+$) were used at an MOI of 10:1. The significance of differences between 2G2 and WT survival, recorded with bacterial CFU at days 3 and 5 of infection, was $P < 0.01$ (**).

tiapoptotic behavior of *M. tuberculosis* (15). We demonstrated that *M. tuberculosis* is capable of blocking the extrinsic pathway of apoptosis by secreting the Rv3654c and Rv3655c effectors, which alter the caspases' posttranscriptional events (15). We also identified the secreted Rv3364c protein, which inhibits caspase-1 activation and consequently host cell apoptosis (pyroptosis) through suppression of the enzymatic activity of cathepsin G (16). In the present study, we characterized the function of the Rv3354 gene and demonstrated for the first time the novel virulence mechanism of *M. tuberculosis* in which the secreted Rv3354 exploits the host ubiquitylation system by altering COP9 signalosome function to limit the degradation of *M. tuberculosis* effector proteins.

RESULTS

Characterization of the Rv3354 gene knockout mutant. The 2G2 mutant (Fig. 1A), which lacks the ability to inhibit macrophage apoptosis, was identified from a transposon bank of *M. tuberculosis* mutants (15). Sequencing analysis revealed that transposon insertion at the 105-amino-acid (aa) site disrupted proper translation of Rv3354 (Fig. 1B). Bioinformatic analysis of the Rv3354 protein revealed domains of DUFF732 (unknown function) and PKc_MEK1 (the catalytic domain of the dual-specificity protein kinase mitogen-activated protein kinase/extracellular signal-regulated kinase 1 [MAPK/ERK1]). Using the sequenced-based prediction for secreted proteins and SignalP 4.1, the presence of a 32-aa signal peptide and export via the Sec system were predicted for Rv3354. Complementation of the 2G2 mutant (Rv3354$^+$) restored the antiapoptotic phenotype (Fig. 1C). We next examined 2G2 for survival in THP-1 cells. *In vitro* studies revealed no difference between growth of *M. tuberculosis* H37Rv wild type (WT) and growth of 2G2 in liquid culture medium (Fig. 1D); however, the Rv3354 knockout clone showed a significant decrease in growth within macrophages (Fig. 1E). The viability was fully recovered by complementing 2G2 with the functional Rv3354 gene. Table 1 shows the comparison in apoptosis and intracellular bacterial growth for the *M. tuberculosis*-infected primary macrophage cell line. The results confirmed that apoptosis and bacterial growth happen in monocyte-derived macrophages (MDM) in a similar way as in THP-1 cells.

The Rv3354 protein is secreted within human macrophages. We recently established a fluorescent screening tool for mycobacterium-secreted proteins by using a TEM-1

TABLE 1 Comparison of the level of apoptosis and intracellular *M. tuberculosis* growth in infected human MDM

	% Apoptosis[b]			CFU/ml of lysate		
Infection[a]	1 day	3 days	5 days	1 day	3 days	5 days
WT	8 ± 3	15 ± 4	38 ± 2	5.9×10^5	2.7×10^6	3.4×10^6
2G2	11 ± 3	35 ± 1	55 ± 4	5.7×10^5	8.9×10^5	1.6×10^6
2G2 (Rv3354$^+$)	9 ± 2	18 ± 3	37 ± 5	5.4×10^5	2.3×10^6	3.6×10^6
No infection	3 ± 1	5 ± 3	14 ± 2			

[a] Approximately 5×10^5 macrophages were infected with *M. tuberculosis* at an MOI of 10.

[b] The results represent the means ± SD of two assays and were determined in an ELISA.

β-lactamase reporter enzyme (Bla) and a mammalian fluorescence resonance energy transfer (FRET)-based probe which can be used to monitor Bla enzyme activity in cultured cells. The positive-control *bla*$^+$ vector with a full-length β-lactamase gene, the negative-control *bla*-deficient vector lacking a signal sequence of the *bla* gene important for β-lactamase enzyme secretion, and the experimental vector containing an Rv3354:*bla*-deficient fusion were transformed into the *M. tuberculosis* β-lactam-sensitive PM638 clone. Bla protein secretion was monitored in THP-1 cells via hydrolysis of the FRET-based β-lactamase substrate CCF2-AM by using fluorescence microscopy (Fig. 2A) as well as a cytofluorometer (Fig. 2B). The infection rate of *M. tuberculosis*-infected THP-1 cells was found to be similar in all groups (Fig. 2C).

Effector Rv3354 interacts with the metalloprotease (JAMM) domain of CSN5. To identify the host protein(s) targeted by the effector Rv3354, we performed a yeast two-hybrid screen with a human universal cDNA library and with the *M. tuberculosis* target protein as the bait. Out of 2×10^7 transformants screened, 21 clones grew in the absence of tryptophan (-Trp), leucine (-Leu), histidine (-His), and adenine (-Ade). Eighteen clones were further eliminated through screening on 125 ng/ml aureobasidin plates in the presence of 5-bromo-4-chloro-3-indolyl-α-galactopyranoside (X-α-Gal) and absence of Ade, His, Leu, and Trp. Three interacting positive clones were sequenced and, two out-of-frame clones were further eliminated. A 48- to 261-aa coding sequence of CSN5 was identified as an interacting partner with Rv3354, and at 68- to 154-aa JAMM domain sequence was detected (Fig. 3A). Further studies using full and reverse constructs of the bait and prey targets confirmed a positive interaction between JAMM and Rv3354 (Fig. 3B, panels a and b). When we mutated JAMM (mJAMM) in the amino acid sequences essential for its metalloprotease activity, neither bait nor pray constructs showed a positive interaction, suggesting that JAMM is a specific target for the *M. tuberculosis* effector.

The effector Rv3354 colocalizes and binds to CSN5 in THP-1 cells. To demonstrate direct binding of Rv3354 to JAMM, we an-

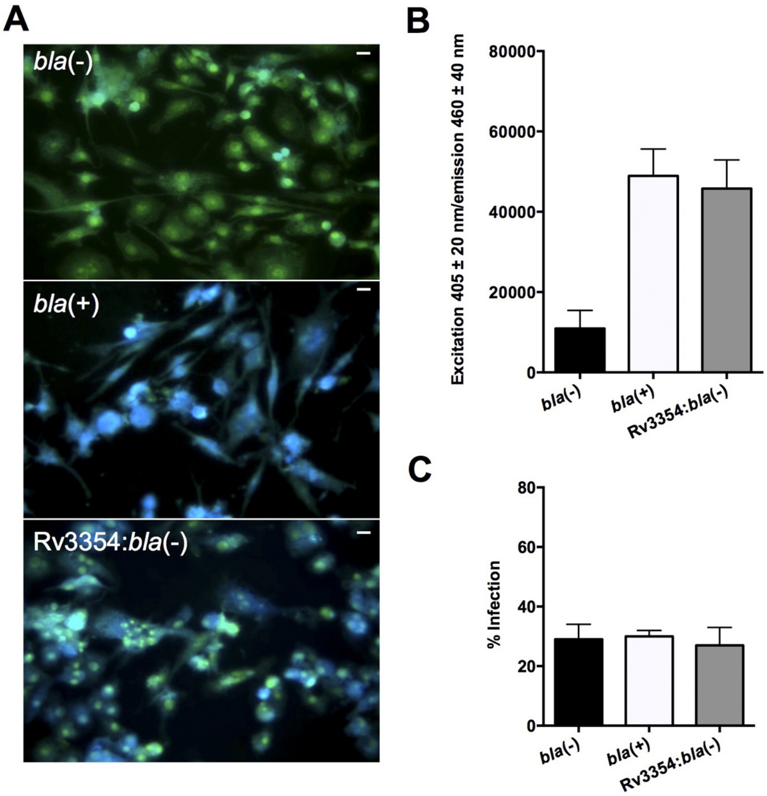

FIG 2 Rv3354 protein secretion within THP-1 cells. (A) THP-1 monolayers in a 96-well plate were loaded with CCF2-AM and then infected with *M. tuberculosis* expressing *bla*-deficient, *bla*$^+$, or Rv3354c:*bla*-deficient vector at an MOI of 10:1. While uncleaved substrate emits green, β-lactamase-catalyzed substrate fluoresces blue. Bar, 10 μm. (B) CCF2-AM hydrolysis readings from THP-1 cells infected with *M. tuberculosis bla*-deficient, *bla*$^+$, or Rv3354c:*bla*-deficient vector also confirmed the robust changes between control and experimental groups, which were recorded with a plate reader. The secretion of β-lactamase was captured at 8 h postinfection. (C) The percentage of *M. tuberculosis*-infected macrophages as a function of the number of ingested *M. tuberculosis* with *bla*-deficient, *bla*$^+$, or Rv3354c:*bla*-deficient vector after 1 h of incubation.

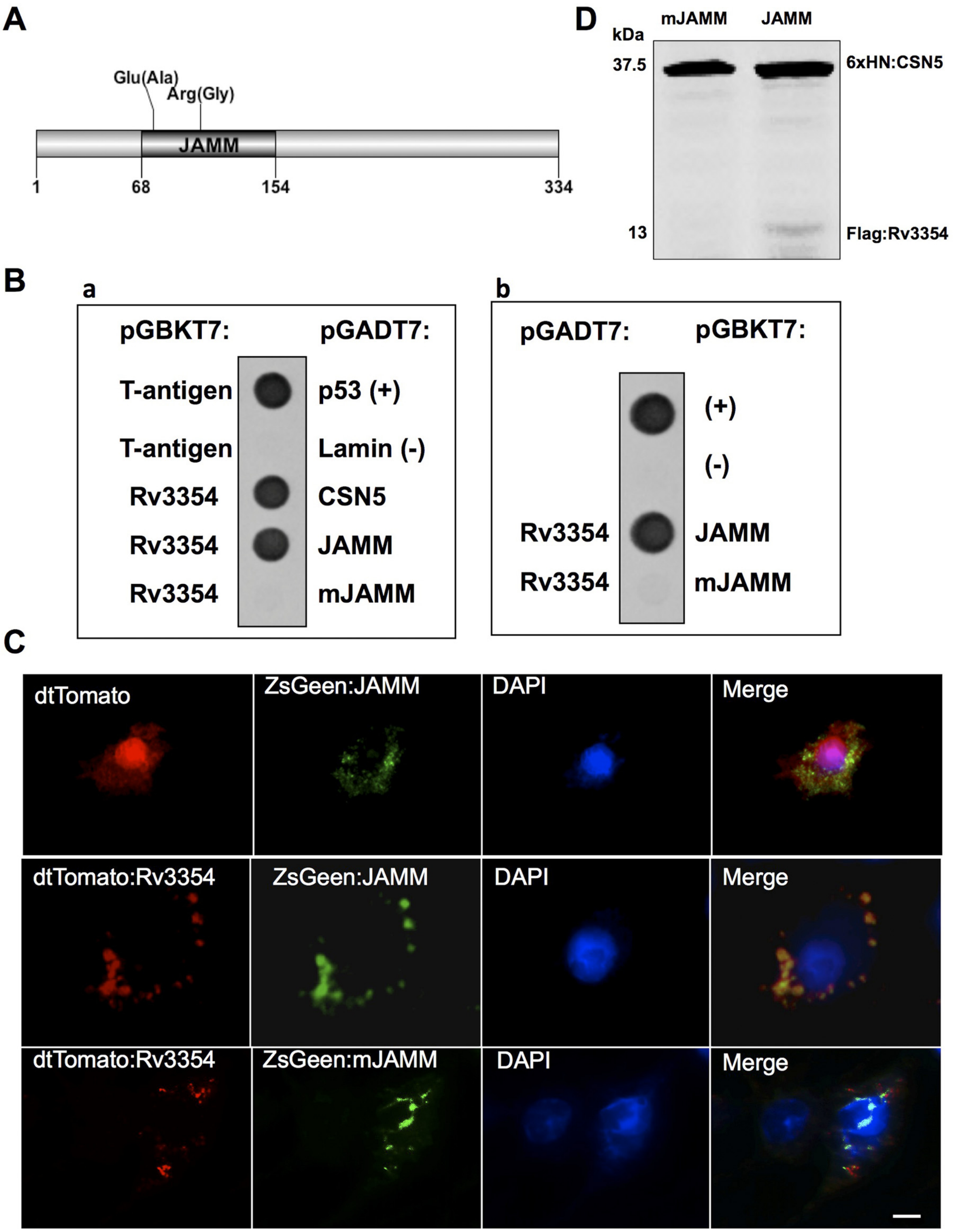
A
Glu(Ala)
Arg(Gly)
JAMM
1
68
154
334
D
kDa
mJAMM
JAMM
37.5
13
6xHN:CSN5
Flag:Rv3354
B
a
pGBKT7:
pGADT7:
T-antigen
p53 (+)
T-antigen
Lamin (-)
Rv3354
CSN5
Rv3354
JAMM
Rv3354
mJAMM
b
pGADT7:
pGBKT7:
(+)
(-)
Rv3354
JAMM
Rv3354
mJAMM
C
dtTomato
ZsGeen:JAMM
DAPI
Merge
dtTomato:Rv3354
ZsGeen:JAMM
DAPI
Merge
dtTomato:Rv3354
ZsGeen:mJAMM
DAPI
Merge

FIG 3 *In vitro* interaction between Rv3354 and CSN5 proteins. (A) Predicted JAMM domain and mutated sites in the CSN5 protein. The amino acids Glu^{77} and Arg^{106}, responsible for metalloprotease activity of CSN5, were replaced with Ala and Gly by using a site-directed QuikChange mutagenesis kit according to the manufacturer's protocol (Stratagene). (B) The yeast two-hybrid interaction of Rv3354 with the host target protein. (a) The full-length CSN5 and, mainly, its JAMM domain showed a positive interaction with Rv3354. (b) Reverse screening of the Rv3354 interaction with JAMM or mJAMM. (C) Subcellular localization of Rv3354 and the JAMM motif of CSN5 in THP-1 cells. dtTomato:Rv3354 and ZsGreen:JAMM viral particles were coexpressed transiently in THP-1 cells for 24 h. Nuclei were stained with 4,6-diamidino-2-phenylindole (DAPI). Bar, 10 μm. (D) Coimmunoprecipitation of Rv3354 and CSN5 proteins. The recombinant 6×HN:CSN5 or mutated version of a protein was incubated with purified *M. tuberculosis* proteins overexpressing Rv3354 with Flag tag. The bound proteins were captured with His columns and subjected to IB with 6×HN and Flag antibodies.

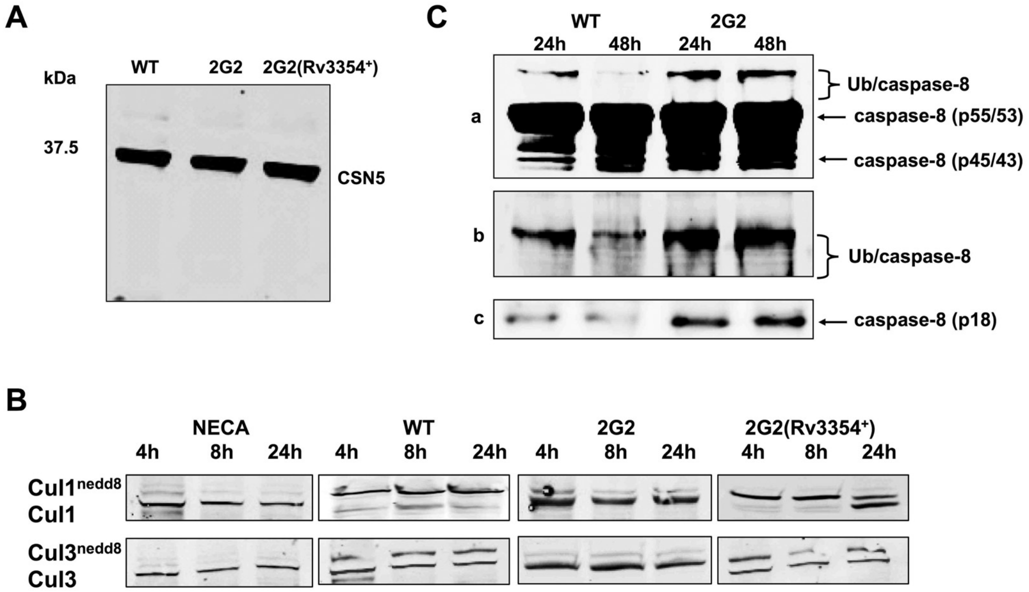

FIG 4 Downstream pathways of CSN5 affected by Rv3354. (A) THP-1 cells were infected with WT, 2G2, and 2G2 (Rv3354$^+$), and after 24 h of infection cell lysates were immunoblotted and probed with an anti-CSN5 antibody. (B) THP-1 cells were treated with 50 μM NECA or infected for up to 24 h with WT, 2G2, and 2G2(Rv3354$^+$), and deneddylation of Nedd8 was assessed by IB using anti-Cul1 and Cul3 antibodies. (C) Caspase-8 polyubiquitination in 2G2-infected cells. THP-1 cells, infected with WT or the 2G2 mutant for up to 48 h, were lysed in sample buffer containing 1% Triton X-100 and cleared by centrifugation. Samples were subjected to caspase-8 immunoprecipitation under denaturing conditions by using an agarose-conjugated primary antibody and analyzed via caspase-8 (a), Ub (b), or p18 (c) IB.

alyzed bacterial and host protein colocalization within macrophages by using a lentiviral transfection system (Fig. 3C) and performed a coimmunoprecipitation assay (Fig. 3D). Following infection of THP-1 cells with lentiviral particles of the fusions tdTomato:Rv3354 and ZsGreen:JAMM or ZsGreen:mJAMM, samples were analyzed with fluorescence microscopy. ZsGreen:JAMM-expressing cells showed granular fluorescence in the cytosol and mainly colocalized with dtTomato:Rv3354-expressing cells, as shown in the merged image in Fig. 3C. Conversely, mutated ZsGreen:mJAMM-expressing cells showed diffuse and uniform cytoplasmic staining with the Rv3354 protein. The control interaction between tdTomato and ZsGreen:JAMM displayed a dispersed location as well.

We also performed coimmunoprecipitation of Flag-tagged Rv3354 (Flag:Rv3354) with 6×HN-tagged CSN5 (6×HN:CSN5). Recombinant 6×HN:CSN5 with or without mutations in JAMM was expressed in the pET system. The Flag:Rv3354 fusion was overexpressed in pMV261 and transformed into *M. tuberculosis*. Bacteria were lysed at the mid-log growth phase, and the cleared protein fraction was incubated with the recombinant 6×HN:CSN5 fusion overnight at 4°C. The CSN5 protein was purified using His columns, and bound proteins were visualized with 6×HN and Flag antibodies by Western blotting. The mutated recombinant 6×HN:mCSN5 protein was used as a negative control in these experiments. Purification of CSN5 led to copurification of Rv3354 (Fig. 3D). No interaction was detected between mutated CSN5 and Rv3354, explaining the lack of physical binding between host and bacterial proteins.

Rv3354 binding to JAMM alters the function of Cullin-based E3 ubiquitin ligases. To examine if the Rv3354 interaction with CSN5 leads to any modification of the host protein, we performed Western blot analysis of CSN5 on whole-cell lysates of THP-1 macrophages infected with the WT, 2G2 mutant, or a complemented clone. We did not observe any cleavage or changes in the molecular mass of CSN5 (Fig. 4A). Next, we asked whether the interaction of Rv3354 with the metalloprotease domain altered CSN5 function. JAMM directly binds to the Nedd8 protein, a key facilitator of ubiquitin-protein isopeptide ligase (E3) complex assembly, and it cleaves Nedd8 from Cul-RING E3 ligases, a process known as deneddylation (17). This process is essential for efficient recycling progression by E3 enzymes. The Western blot analysis of cullin1 (Cul1), cullin3 (Cul3), and associated Nedd8 protein was carried out in WT-, 2G2- or 2G2 (Rv3354$^+$)-infected macrophages. As shown in Fig. 4B, while immunoblotting (IB) of Cul1 and Cul3, derived from 2G2-infected THP-1 cells, revealed a nearly complete deneddylation of Cul1 and Cul3 at all time points, the wild-type and complemented 2G2 infections partially blocked the deneddylation process. The loss of Nedd8 was apparent in the positive-control group, which was cells treated with 50 μM *N*-ethyl-carbamidoadenosine (NECA) (Fig. 4B).

Modification of Cul3-based E3 ubiquitin ligase activity mediates caspase-8 inhibition during *M. tuberculosis* infection. The cul3-based E3 ligase interaction with DISC (death-inducing signaling complex) has been demonstrated to induce Cul3-mediated polyubiquitination of caspase-8, promoting its full activation and apoptosis (18). To examine whether alteration in the Cul3 deneddylation process by *M. tuberculosis* results in changes of caspase-8 polyubiquitination and, alternatively, its activation, we performed a caspase-8 immunoprecipitation assay with extracts of THP-1 cells infected with either WT or 2G2 followed by Western blotting with caspase-8 or ubiquitin (Ub) antibody. The results indicated that the amount of ubiquitinated caspase-8 in WT-infected cells markedly decreased at 48 h compared with 2G2 infection (Fig. 4C, panels a and b). The amount of activated p18

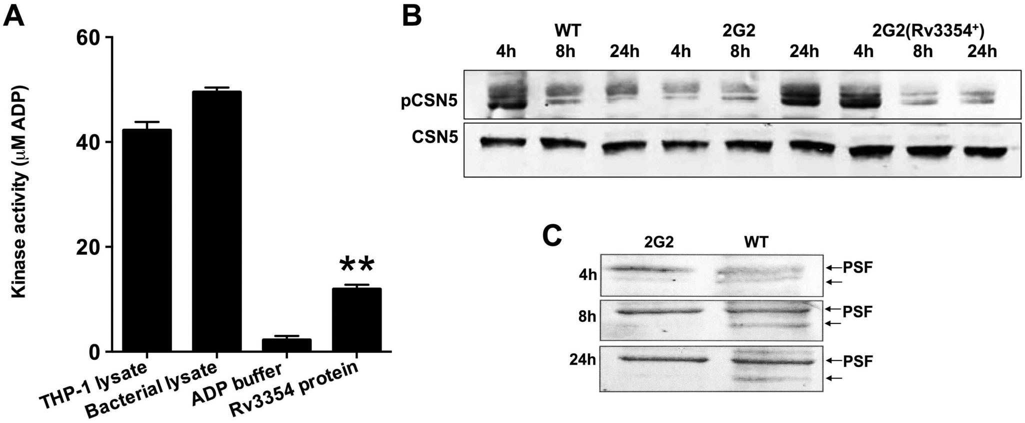

FIG 5 Kinase activity of Rv3354 protein. (A) Kinase activity of recombinant Rv3354 was assessed by fluorescently measuring ADP production as a direct result of kinase phosphotransferase activity from ATP. Results represent means ± standard errors of three independent experiments. **, $P < 0.01$, significance of differences between experimental Rv3354 and the reaction buffer control. (B) THP-1 cells were infected with WT, 2G2, and 2G2 (Rv3354$^+$) for 4, 8, and 24 h, and cleared protein samples were subjected to CSN5 immunoprecipitation using agarose-conjugated primary antibody. Total CSN5 was IB with anti-phosphoserine/threonine/tyrosine antibody. (C) IB analysis of PSF protein in WT- and 2G2-infected macrophages at 4, 8, 12, 24, or 48 h postinfection.

(caspase-8) was significantly lower in WT-infected cells than in 2G2-infected cells at both 24 h and 48 h postinfection (Fig. 4C, panel c).

Rv3354 demonstrates protein kinase activity. Bioinformatic analysis of the Rv3354 protein revealed a catalytic domain of the MAP/ERK1 protein on the C terminus. To determine if Rv3354 possesses any kinase activity, phosphotransferase activity was measured by ADP production. Briefly, ATP, as a kinase substrate, was added to the recombinant 6×HN:Rv3354 protein (200 μg/ml) or bacterial or host total protein extracts (650 μg/ml; positive controls). As shown in Fig. 5A, the experimental wells that contained purified Rv3354 produced significantly more ADP than the reaction buffer (negative control) alone, demonstrating that when ATP is a substrate, the Rv3354 protein possesses kinase activity.

CSN5 has a reduced level of phosphorylation in the absence of Rv3354. To evaluate the effect of Rv3354, as a potential protein kinase, on CSN5 activity, we analyzed CSN5 phosphorylation during *M. tuberculosis* infection. Figure 5B shows increasing amounts of CSN5 at 4 h postinfection in WT- and 2G2 (Rv3354$^+$)-infected macrophages, while 2G2-infected cells had significantly lower CSN5 protein levels at 4 h and 8 h postinfection. Over time, the phosphorylation of CSN5 markedly decreased in H37Rv- and 2G2 (Rv3354$^+$)-infected cells, whereas CSN5 phosphorylation levels increased in 2G2 mutant-infected cells at 24 h postinfection (Fig. 5B).

Modulation of CSN5 function most likely protects *M. tuberculosis* effectors from Ub degradation. The most-characterized biological process that the COP9 signalosome regulates via JAMM of CSN5 is the cleavage of the ubiquitin-like protein Nedd8 from Cul-containing E3 ligases. The neddylation and deneddylation of cullins are needed to sustain E3 ligase activities, which attach ubiquitin to target proteins for proteasome-mediated degradation. We next asked whether Rv3354 binding to JAMM and its interference with E3 ligase activity was a strategy of the bacterium to avoid ubiquitination of its effector proteins. To further examine this possibility, we infected cells with WT and 2G2 and performed IB analysis for the polypyrimidine tract-binding protein-associated splicing factor (PSF). Previously, we demonstrated that the antiapoptotic secreted Rv3654c protein, nonfunctional in the 31G12 clone, binds to the PSF in macrophages and cleaves the host protein. This, in turn, results in decreased levels of caspase-8 activity, which leads to inhibition of the intrinsic pathway of apoptosis (15). In the current study, we observed that the 2G2 mutant, in contrast to WT infection but similarly to infection with the Rv3654c knockout clone (31G12), failed to cleave the PSF protein (Fig. 5C). Our observation suggests the possibility that the Rv3654c effector is degraded in cells infected with 2G2 (lacking Rv3354) and, as a result, fails to cleave PSF.

DISCUSSION

Host-driven apoptotic death of macrophages during bacterial infection appears to be an essential aspect of innate immunity aimed at the elimination of niche cells on which bacteria rely for replication and survival (19). Modulation of apoptosis is one of the mechanisms whereby *M. tuberculosis* avoids death by macrophages (20). Less is known about the *M. tuberculosis* virulence factors that are involved in control of the apoptosis process, although *M. tuberculosis* antiapoptotic phenotypes in host cells have been well documented (11, 19, 20) and *de novo* protein synthesis has been suggested to control an antiapoptotic activity in both macrophages and epithelial cells (11). We identified an *M. tuberculosis* transposon clone with a nonfunctional Rv3354 gene as deficient in the inhibition of macrophage apoptosis and observed that Rv3354 is required for *M. tuberculosis* virulence and survival in macrophages. By constructing the Rv3354 signal sequence fusion with the β-lactamase reporter gene and utilizing the mammalian cell-based reporter assay, we demonstrated Rv3354 protein secretion within THP-1 phagocytic cells. Complementary to our findings, other groups have shown Rv3354 protein export in culture filtrates of *M. tuberculosis* H37Rv and experimentally confirmed its secretion via a phoA′ reporter system *in vitro* (21, 22). Furthermore, protein-protein interaction studies identified the metalloprotease (JAMM) motif within CSN5 as an interacting partner for Rv3354. CSN is implicated in diverse biological functions, including apoptosis (23). In particular, when CSN5, an essential subunit for CSN metalloprotease activity, is deleted from the COP9 complex, it leads to apoptotic cell death *in vivo* (23). In addition, CSN5 can stably exist independently from the complex.

As an independent apoptotic mechanism from CSN, CSN5 can enhance apoptosis via activation of transcription factor E2F1 (23). CSN5 regulates the cullin-ring ligase (CRL) families of ubiquitin E3 complexes by cleaving (via deneddylation) a ubiquitin-like protein, Nedd8, from the cullin ring. Many bacterial pathogens have developed diverse strategies of interference with the host ubiquitin-proteasome system and, in several cases as a consequence, alter the apoptosis process (24, 25). Evidence suggests that effector proteins such as NleG (*Escherichia coli* O157:H7), LubX and SidH (*Legionella pneumophila*), SopA and SspH2 (*Salmonella*), and IpaH3 (*Shigella*) mimic and function as E3 ubiquitin ligases in the host (24). In contrast, effectors like SseL (*Salmonella*), TssM (*Burkholderia pseudomallei*), YopJ (*Yersinia pseudotuberculosis* and *Yersinia pestis*), and YopP (*Yersinia enterocolitica*) exhibit deubiquitylation activities that manipulate regulatory components of the host ubiquitin system and apoptosis (25, 26). In some cases, as a part of the intracellular activation mechanism of effector proteins, for example, with ExoU (*Pseudomonas*), the host ubiquitin is used as a cofactor for enzymatic activation (27). In this work, we have provided evidence that *M. tuberculosis*-secreted protein Rv3354 possesses protein kinase activity, and we have demonstrated that the interaction of Rv3354 with the JAMM motif changes a phosphorylation profile of CSN5 in *M. tuberculosis*-infected cells. The recent work has implicated a functional relationship between the CSN and protein kinase enzymes, and this relationship determines CSN stability toward the ubiquitin system. In fact, immunoprecipitation and far-Western blotting experiments have revealed that CSN copurifies with protein kinases and serves as a docking site for the phosphorylation of various substrates (28). Analysis of CSN5-associated kinase-specific phosphorylation sites has revealed several serine and threonine residues as putative phosphate acceptors, and mutations in these sites have confirmed its importance in activation of CSN (17, 29). In addition, the treatment of cultured cells with the piceatannol, an inhibitor of CSN-associated kinases, has an effect on CSN5 function (30). A genetic inactivation of the Rv3354 gene leads to decreased activation of CSN, which is normally enhanced with the wild-type *M. tuberculosis*. The significant phosphorylation of CSN5 at early time points suggests that the pathogen attempts to inactivate the proteasome system by blocking the deneddylation process of enzymes that is responsible for enabling this system. Our results demonstrate that the most prominent Cul1 and Cul3 ligases of CSN in WT-infected cells lead to accumulation of Nedd8-conjugated enzymes. In addition, it has been established that p62-dependent Cul3-mediated polyubiquitination and activation of caspase-8 mediate extrinsic apoptosis signaling (18). We found that when the Rv3354 knockout mutant failed to destabilize the Cul3 enzyme in a similar manner as the WT, it led to a significantly higher level of caspase-8 polyubiquitination. Similar to *M. tuberculosis*, the Vpr protein of human immunodeficiency virus type 1 (HIV-1) has been implicated in regulation of apoptosis via interaction with CSN (31). Alternatively, the cycle-inhibiting factors (Cif) of many pathogenic bacteria have been shown to directly interact with several Nedd8-conjugated cullins and to inhibit ubiquitin ligase activity, altering 26S proteasome-mediated degradation (32).

Why would a pathogen target host ubiquitin-mediated protein degradation? Recent reports suggest that bacterial modulation of the host proteasome system is a mechanism to program the elimination of effector proteins when the bacterium's function within the host cell is no longer required, therefore avoiding permanent damaging effects in the host cell (26). In fact, certain pathogens modulate this system to temporarily prevent the destruction of active effectors. This strategy also ensures safe synthesis and efficient export of secreted proteins into the host cells. For example, temporal regulation has been reported for *Salmonella* Rho GTPase-modulating enzymes, SopE and SptP, and for *Legionella pneumophila* E3 ligases LubX and SidH (27). Our hypothesis is that by modifying the signalosome function, *M. tuberculosis* might also enhance the activity of many other effector proteins delivered to host cells at the same time as Rv3354. In this work, by using the Rv3354 knockout mutant, we demonstrated that *M. tuberculosis* fails to cleave the host PSF protein in a similar fashion as the 31G12 knockout mutant of the Rv3654c gene (15). This observation suggests that when *M. tuberculosis* fails to impair CSN activity, secretion of the Rv3654c effector (responsible for direct modification of PSF) is inefficient, most likely due to protein degradation.

The successful reprogramming of cellular survival or death pathways by *M. tuberculosis*, which influences host immune responses, has been mainly justified through the ESX-1 secretion system and its ESAT-6 and CFP-10 effectors. However, recent evidence shows that blocking the secretion of these effectors does not always result in *M. tuberculosis* attenuation *in vitro* and *in vivo* (33). A growing literature has revealed new virulence factors that influence the intracellular survivability of *M. tuberculosis*. In the current study, we characterized the Rv3354 virulence effector that is required for *M. tuberculosis* survival in macrophages. The underlying mechanism of the Rv3354-CSN5 interaction as a cause of apoptosis remains unclear; however, an indirect mechanism cannot be excluded at this time. Based on our work, we can conclude that *M. tuberculosis* alters the CSN function and limits E3 ligase activity via Rv3354, and this possibly prevents the ubiquitin-mediated protein degradation of *M. tuberculosis* effector proteins. This finding adds another layer of complexity to *M. tuberculosis* virulence and provides insight into future research that will help to elucidate a novel mechanism of *M. tuberculosis* pathogenicity.

MATERIALS AND METHODS

Antibodies and systems. The primary antibodies against CSN5, Cul1, Cul3, caspase-8, Ub, PSF, β-actin, phosphoserine/threonine/tyrosine of human origin, and Flag and 6×HN probes were purchased from Santa Cruz Biotechnology. All chemicals were obtained from Sigma. The GeneBLAzer cell-based assay loading kit was from Life Technologies. The yeast two-hybrid Normalized Mate and Plate universal human library, the yeast transformation system, and the bait, prey, and control vectors were obtained from Clontech. The Lenti-X lentiviral expression system was also purchased from Clontech.

Cell and bacterial cultures. The THP-1 human monocyte cell line was obtained from the American Type Culture Collection (ATCC) and maintained in RPMI 1640 medium (Lonza) supplemented with heat-inactivated 10% fetal bovine serum (FBS) and 2 mM L-glutamine. To promote maturation and adherence, cells were treated with 100 ng/ml of phorbol 12-myristate 13-acetate (PMA; Sigma Aldrich) and then seeded at 80% confluence into 75-cm^2 tissue culture flasks, 24-well plates, or chamber glass slides, as needed. After 24 h, cells were replenished with new medium and incubated for an additional 48 h for cell differentiation. The *M. tuberculosis* 2G2 mutant, 2G2 (Rv3354$^+$), and wild-type H37Rv, purchased from ATCC, were grown until mid-exponential phase in Middlebrook 7H9 broth supplemented with 10% albumin-dextrose-catalase, 0.2% glycerol, and 0.05% Tween 80. Where appropriate, kanamycin was added at a concentration of 200 μg/ml. *M. tuberculosis* cells were homogenized to remove clumps, and only dispersed inocula were used in infection experiments. The viable counts of inocula were determined by serial dilution and plating on 7H11 agar with 10% oleic acid-albumin-dextrose-catalase. Human MDM were obtained from the blood of volunteers by using protocols approved by the Institutional Human Subject Committee. The purification, culture, and maturation of these cells were described previously (34). Cells were cultured in RPMI 1640 medium supplemented with 10% autologous serum. In all experiments, macrophages were infected at a multiplicity of infection (MOI) of 10. CFU were calculated at different times postinfection. In another set of experiments, apoptosis was measured via a cell death detection enzyme-linked immunosorbent assay (ELISA^{PLUS}; Roche) or cells were cleared and analyzed by Western blotting for selected host proteins.

Complementation of 2G2. The PCR-generated 390-bp coding fragment of Rv3354 was cloned into the mycobacterium shuttle vector pMV261-AprII containing the apramycin resistance marker. The resulting vector was electroporated into 2G2. Transformants were plated on agar plates containing 200 μg/ml of apramycin and screened for positive clones by PCR using apramycin primers (15).

β-Lactamase assay for protein secretion. A 32-aa coding sequence of the Rv3354 gene was cloned into the mycobacterium-*E. coli* shuttle vector pLDG13 downstream of the G13 promoter of *Mycobacterium marinum* and upstream of the *bla* gene lacking the first 69-bp signal sequence. The resultant vector was transformed into the *bla*C knockout strain PM638 of *M. tuberculosis* H37Rv. Approximately 10^5 THP-1 cells were seeded into 96-well plates or in 2-chamber slides and infected with *M. tuberculosis* clones expressing the full-length *bla*$^+$, the *bla*-deficient mutant missing the signal sequence, or the Rv3354:*bla*-deficient fusion. After a 1-h incubation at 37°C in 5% CO_2, extracellular bacteria were removed by washing wells with Hanks' balanced salt solution. Infected control and experimental monolayers were loaded with the cell-permeable dye CCF2-AM using the manufacturer's protocol (Life Technologies). Readings were recorded with a Tecan Infinite 200 microplate reader with two filter sets with excitation at 405 ± 20 nm and emission at 460 ±40 nm or excitation at 405 ± 20 nm and emission at 530 ±30 nm. Fluorescence micrographs were captured with a Leica DM4000B microscope.

Matchmaker Gold yeast two-hybrid screening. The Rv3354 gene was cloned in frame with the GAL4 DNA binding domain of pGBKT7. The resultant pGBKT7:Rv3354 vector was transformed into *Saccharomyces cerevisiae* strain Y2HGold following the manufacturer's instructions (Clontech). The normalized yeast two-hybrid universal human library, fused with the GAL4 activation domain of the pGADT7 vector and stored in the Y187 yeast strain, was purchased from Clontech. The interaction between pGBKT7-53 and pGADT7-T served as a positive control, whereas pGBKT7-lam and pGADT7-T were used as a control for a negative interaction. One milliliter of the library was combined with 4 ml of a bait yeast strain and grown in 2× yeast extract-peptone-dextrose-adenine liquid medium containing 50 μg/ml kanamycin at 30°C for 24 h with slow shaking (50 rpm). Zygotes were plated on double (SD-Leu/-Trp), triple (SD-His/-Leu/-Trp), and quadruple (SD-Ade/-His/-Leu/-Trp) dropout agar plates with or without 20 mg/ml of X-α-Gal and 125 ng/ml aureobasidin. Colonies that turned blue were PCR amplified using the Matchmaker Insert Check PCR Mix 2 system (Clontech), and resulting products were sequenced at the CGRB facility of Oregon State University.

Lentiviral gene transfer and coexpression. To enhance the efficient cotransduction and expression of bacterial and host proteins in THP-1 cells, we used the lentiviral expression system (Clontech). The coding sequence of Rv3354 was cloned into the pLVX-tdTomato-C1 (dtTomato) vector. *Homo sapiens* first-strand cDNAs from total RNA were synthesized using the SuperScript III first-strand synthesis system (Life Technologies). The JAMM sequence of the CSN5 gene was amplified from the synthesized cDNA and cloned into the pLVX-ZsGreen1-C1 vector. Generated lentiviral constructs (tdTomato:Rv3354 and ZsGreen:JAMM) were transiently transfected along with the Lenti-X HTX packaging mix (Clontech) into Lenti-X 293T packaging cells to produce high-titer infectious viral stocks. After 72 h of budding, lentiviruses were purified from the cell supernatants and titers were determined according to the manufacturer's protocol (Clontech).

THP-1 cells were differentiated in 8-chamber slides, supplemented with 4 μg/ml polybrene, and infected with tdTomato:Rv3354 and ZsGreen:JAMM simultaneously. After 24 h, cells were assessed for Tomato and ZsGreen protein colocalization by immunofluorescence microscopy. Coexpression of tdTomato and ZsGreen:JAMM or of dtTomato:Rv3354 and ZsGreen:mJAMM (containing a mutated domain) were used as controls for colocalization studies.

Coimmunoprecipitation. The CSN5 protein with or without mutations in the JAMM domain was expressed in the pET6×HN-C vector (Clontech) in *E. coli* and purified with a His column according to the manufacturer's protocol (Clontech). Alternatively, *M. tuberculosis* expressing Flag:Rv3354 in pMV261 was lysed by mechanical disruption. The purified CSN5 protein was incubated with lysate of *M. tuberculosis* cells expressing Rv3354. After overnight incubation at 4°C, samples were loaded into His columns, washed, and eluted. Proteins of interest were visualized with Western blotting using 6×HN and Flag antibodies.

Western blotting. Uninfected or WT-, 2G2-, or 2G2 (Rv3354$^+$)-infected THP-1 cells after 8, 24, or 48 h were lysed in CelLytic M lysis buffer supplemented with protease inhibitor cocktail (Sigma). Samples were centrifuged at 10,000 × *g* for 15 min to remove the bacterial pellet and cell debris and then solubilized in the sample buffer (Bio-Rad). Precleared samples were separated on 12% Tris-HCl gels and transferred to nitrocellulose. Membranes were blocked with 3% bovine serum albumin (BSA) in PBS containing 0.1% Tween for 1 h and then incubated with primary antibody at a 1:250 dilution for 1 h. Next, membranes were probed with the corresponding IRDye secondary antibody (Li-Cor Biosciences, Inc.) at a dilution of 1:5,000 for 30 min, and proteins were detected using an Odyssey Imager (Li-Cor).

Protein kinase activity assessment. The Universal fluorometric kinase assay kit (Abcam) was used to monitor the phosphotransferase activity of the Rv3354 protein. Briefly, 5 ml of purified 6×HN:Rv3354 was dialyzed and concentrated in 3-kDa centrifugal columns (Pall). Fifty-microliter aliquots of kinase reaction mixtures were set up with 20 μl of ADP buffer, 25 μl of lysate/purified Rv3354/H_2O, and 5 μl of 1 mM ATP or H_2O and incubated at 37°C for 30 min. Twenty microliters of the kinase reaction mixture was combined with 20 μl of ADP sensor buffer and 10 μl of ADP sensor and the mixture was incubated in the dark for 15 min. The standard curve was also created and used as a reference to determine ADP production from samples. Fluorescent readings were taken with a Tecan reader using excitation at 530 nm/emission at 590 nm.

Statistics. Statistical analysis results are presented as means ± standard deviations (SD) of results from two independent replicates unless otherwise indicated. The significance level was determined by using Student's *t* test. A *P* value of <0.05 was considered statistically significant.

ACKNOWLEDGMENTS

We thank Martin Pavelka at the University of Rochester for providing *M. tuberculosis* strain PM638.

This work was supported by the Foundation for Microbiology and National Institutes of Health award 1RO1AI47010.

REFERENCES

1. **Hou JM, D'Lima NG, Rigel NW, Gibbons HS, McCann JR, Braunstein M, Teschke CM.** 2008. ATPase activity of *Mycobacterium tuberculosis* SecA1 and SecA2 proteins and its importance for SecA2 function in macrophages. J. Bacteriol. **190:**4880–4887. http://dx.doi.org/10.1128/JB.00412-08.
2. **Tan T, Lee WL, Alexander DC, Grinstein S, Liu J.** 2006. The ESAT-6/CFP-10 secretion system of Mycobacterium marinum modulates phagosome maturation. Cell. Microbiol. **8:**-1417–1429. http://dx.doi.org/10.1111/j.1462-5822.2006.00721.x.
3. **Vergne I, Chua J, Lee HH, Lucas M, Belisle J, Deretic V.** 2005. Mechanism of phagolysosome biogenesis block by viable *Mycobacterium tuber-*

culosis. Proc. Natl. Acad. Sci. U. S. A. **102:**4033–4038. http://dx.doi.org/10.1073/pnas.0409716102.

4. **Bach H, Papavinasasundaram KG, Wong D, Hmama Z, Av-Gay Y.** 2008. *Mycobacterium tuberculosis* virulence is mediated by PtpA dephosphorylation of human vacuolar protein sorting 33B. Cell Host Microbe **3:**316–322. http://dx.doi.org/10.1016/j.chom.2008.03.008.
5. **Axelrod S, Oschkinat H, Enders J, Schlegel B, Brinkmann V, Kaufmann SH, Haas A, Schaible UE.** 2008. Delay of phagosome maturation by a mycobacterial lipid is reversed by nitric oxide. Cell. Microbiol. **10:**1530–1545. http://dx.doi.org/10.1111/j.1462-5822.2008.01147.x.
6. **Alonso S, Pethe K, Russell DG, Purdy GE.** 2007. Lysosomal killing of Mycobacterium mediated by ubiquitin-derived peptides is enhanced by autophagy. Proc. Natl. Acad. Sci. U. S. A. **104:**6031–6036. http://dx.doi.org/10.1073/pnas.0700036104.
7. **Gutierrez MG, Master SS, Singh SB, Taylor GA, Colombo MI, Deretic V.** 2004. Autophagy is a defense mechanism inhibiting BCG and *Mycobacterium tuberculosis* survival in infected macrophages. Cell **119:**753–766. http://dx.doi.org/10.1016/j.cell.2004.11.038.
8. **Romagnoli A, Etna MP, Giacomini E, Pardini M, Remoli ME, Corazzari M, Falasca L, Goletti D, Gafa V, Simeone R, Delogu G, Piacentini M, Brosch R, Fimia GM, Coccia EM.** 2012. ESX-1 dependent impairment of autophagic flux by *Mycobacterium tuberculosis* in human dendritic cells. Autophagy **8:**1357–1370. http://dx.doi.org/10.4161/auto.20881.
9. **Shin DM, Jeon BY, Lee HM, Jin HS, Yuk JM, Song CH, Lee SH, Lee ZW, Cho SN, Kim JM, Friedman RL, Jo EK.** 2010. *Mycobacterium tuberculosis* Eis regulates autophagy, inflammation, and cell death through redox-dependent signaling. PLoS Pathog. **6:**e1001230. http://dx.doi.org/10.1371/journal.ppat.1001230.
10. **Loeuillet C, Martinon F, Perez C, Munoz M, Thome M, Meylan PR.** 2006. *Mycobacterium tuberculosis* subverts innate immunity to evade specific effectors. J. Immunol. **177:**6245–6255. http://dx.doi.org/10.4049/jimmunol.177.9.6245.
11. **Danelishvili L, McGarvey J, Li YJ, Bermudez LE.** 2003. *Mycobacterium tuberculosis* infection causes different levels of apoptosis and necrosis in human macrophages and alveolar epithelial cells. Cell. Microbiol. **5:**649–660. http://dx.doi.org/10.1046/j.1462-5822.2003.00312.x.
12. **Velmurugan K, Chen B, Miller JL, Azogue S, Gurses S, Hsu T, Glickman M, Jacobs WR, Jr, Porcelli SA, Briken V.** 2007. *Mycobacterium tuberculosis* nuoG is a virulence gene that inhibits apoptosis of infected host cells. PLoS Pathog. **3:**e110. http://dx.doi.org/10.1371/journal.ppat.0030110.
13. **Hinchey J, Lee S, Jeon BY, Basaraba RJ, Venkataswamy MM, Chen B, Chan J, Braunstein M, Orme IM, Derrick SC, Morris SL, Jacobs WR, Jr, Porcelli SA.** 2007. Enhanced priming of adaptive immunity by a proapoptotic mutant of *Mycobacterium tuberculosis*. J. Clin. Invest. **117:**2279–2288. http://dx.doi.org/10.1172/JCI31947.
14. **Jayakumar D, Jacobs WR, Jr, Narayanan S.** 2008. Protein kinase E of *Mycobacterium tuberculosis* has a role in the nitric oxide stress response and apoptosis in a human macrophage model of infection. Cell. Microbiol. **10:**365–374. http://dx.doi.org/10.1111/j.1462-5822.2007.01049.x.
15. **Danelishvili L, Yamazaki Y, Selker J, Bermudez LE.** 2010. Secreted *Mycobacterium tuberculosis* Rv3654c and Rv3655c proteins participate in the suppression of macrophage apoptosis. PLoS One **5:**e10474. http://dx.doi.org/10.1371/journal.pone.0010474.
16. **Danelishvili L, Everman JL, McNamara MJ, Bermudez LE.** 2011. Inhibition of the plasma-membrane-associated serine protease cathepsin G by *Mycobacterium tuberculosis* Rv3364c suppresses caspase-1 and pyroptosis in macrophages. Front. Microbiol. **2:**281. http://dx.doi.org/10.3389/fmicb.2011.00281.
17. **Echalier A, Pan Y, Birol M, Tavernier N, Pintard L, Hoh F, Ebel C, Galophe N, Claret FX, Dumas C.** 2013. Insights into the regulation of the human COP9 signalosome catalytic subunit, CSN5/Jab1. Proc. Natl. Acad. Sci. U. S. A. **110:**1273–1278. http://dx.doi.org/10.1073/pnas.1219502110.
18. **Jin Z, Li Y, Pitti R, Lawrence D, Pham VC, Lill JR, Ashkenazi A.** 2009. Cullin3-based polyubiquitination and p62-dependent aggregation of caspase-8 mediate extrinsic apoptosis signaling. Cell **137:**721–735. http://dx.doi.org/10.1016/j.cell.2009.03.015.
19. **Ashida H, Mimuro H, Ogawa M, Kobayashi T, Sanada T, Kim M, Sasakawa C.** 2011. Cell death and infection: a double-edged sword for host and pathogen survival. J. Cell Biol. **195:**931–942. http://dx.doi.org/10.1083/jcb.201108081.
20. **Lee J, Hartman M, Kornfeld H.** 2009. Macrophage apoptosis in tuberculosis. Yonsei Med. J. **50:**1–11. http://dx.doi.org/10.3349/ymj.2009.50.1.1.
21. **Målen H, Berven FS, Fladmark KE, Wiker HG.** 2007. Comprehensive analysis of exported proteins from *Mycobacterium tuberculosis* H37Rv. Proteomics **7:**1702–1718. http://dx.doi.org/10.1002/pmic.200600853.
22. **Gomez M, Johnson S, Gennaro ML.** 2000. Identification of secreted proteins of *Mycobacterium tuberculosis* by a bioinformatic approach. Infect. Immun. **68:**2323–2327. http://dx.doi.org/10.1128/IAI.68.4.2323-2327.2000.
23. **Wei N, Serino G, Deng XW.** 2008. The COP9 signalosome: more than a protease. Trends Biochem. Sci. **33:**592–600. http://dx.doi.org/10.1016/j.tibs.2008.09.004.
24. **Anderson DM, Frank DW.** 2012. Five mechanisms of manipulation by bacterial effectors: a ubiquitous theme. PLoS Pathog. **8:**e1002823. http://dx.doi.org/10.1371/journal.ppat.1002823.
25. **Rytkönen A, Holden DW.** 2007. Bacterial interference of ubiquitination and deubiquitination. Cell Host Microbe **1:**13–22. http://dx.doi.org/10.1016/j.chom.2007.02.003.
26. **Angot A, Vergunst A, Genin S, Peeters N.** 2007. Exploitation of eukaryotic ubiquitin signaling pathways by effectors translocated by bacterial type III and type IV secretion systems. PLoS Pathog. **3:**e3. http://dx.doi.org/10.1371/journal.ppat.0030003.
27. **Anderson DM, Feix JB, Monroe AL, Peterson FC, Volkman BF, Haas AL, Frank DW.** 2013. Identification of the major ubiquitin-binding domain of the Pseudomonas aeruginosa ExoU A2 phospholipase. J. Biol. Chem. **288:**26741–26752. http://dx.doi.org/10.1074/jbc.M113.478529.
28. **Uhle S, Medalia O, Waldron R, Dumdey R, Henklein P, Bech-Otschir D, Huang X, Berse M, Sperling J, Schade R, Dubiel W.** 2003. Protein kinase CK2 and protein kinase D are associated with the COP9 signalosome. EMBO J. **22:**1302–1312. http://dx.doi.org/10.1093/emboj/cdg127.
29. **Bech-Otschir D, Seeger M, Dubiel W.** 2002. The COP9 signalosome: at the interface between signal transduction and ubiquitin-dependent proteolysis. J. Cell Sci. **115:**467–473.
30. **Tanguy G, Drévillon L, Arous N, Hasnain A, Hinzpeter A, Fritsch J, Goossens M, Fanen P.** 2008. CSN5 binds to misfolded CFTR and promotes its degradation. Biochim. Biophys. Acta **1783:**1189–1199. http://dx.doi.org/10.1016/j.bbamcr.2008.01.010.
31. **Muthumani K, Choo AY, Premkumar A, Hwang DS, Thieu KP, Desai BM, Weiner DB.** 2005. Human immunodeficiency virus type 1 (HIV-1) Vpr-regulated cell death: insights into mechanism. Cell Death Differ. **12** (Suppl 1):962–970. http://dx.doi.org/10.1038/sj.cdd.4401583.
32. **Jubelin G, Taieb F, Duda DM, Hsu Y, Samba-Louaka A, Nobe R, Penary M, Watrin C, Nougayrède JP, Schulman BA, Stebbins CE, Oswald E.** 2010. Pathogenic bacteria target NEDD8-conjugated cullins to hijack host-cell signaling pathways. PLoS Pathog. **6:**e1001128. http://dx.doi.org/10.1371/journal.ppat.1001128.
33. **Chen JM, Zhang M, Rybniker J, Basterra L, Dhar N, Tischler AD, Pojer F, Cole ST.** 2013. Phenotypic profiling of *Mycobacterium tuberculosis* EspA point mutants reveals that blockage of ESAT-6 and CFP-10 secretion *in vitro* does not always correlate with attenuation of virulence. J. Bacteriol. **195:**5421–5430. http://dx.doi.org/10.1128/JB.00967-13.
34. **Bermudez LE, Young LS.** 1988. Tumor necrosis factor, alone or in combination with IL-2, but not IFN-gamma, is associated with macrophage killing of Mycobacterium avium complex. J. Immunol. **140:**3006–3013.